

Cell Reports

Supplemental Information

Sorting of Dendritic and Axonal Vesicles

at the Pre-axonal Exclusion Zone

Ginny G. Farías, Carlos M. Guardia, Dylan J. Britt, Xiaoli Guo, and Juan S. Bonifacino

Figure S1

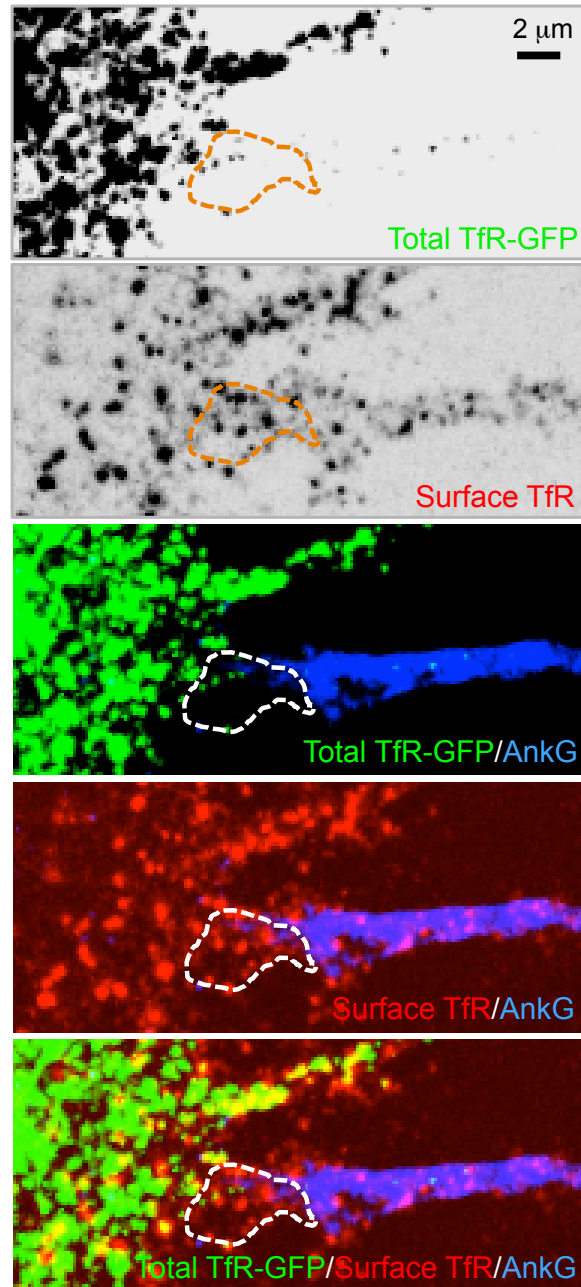


Figure S2

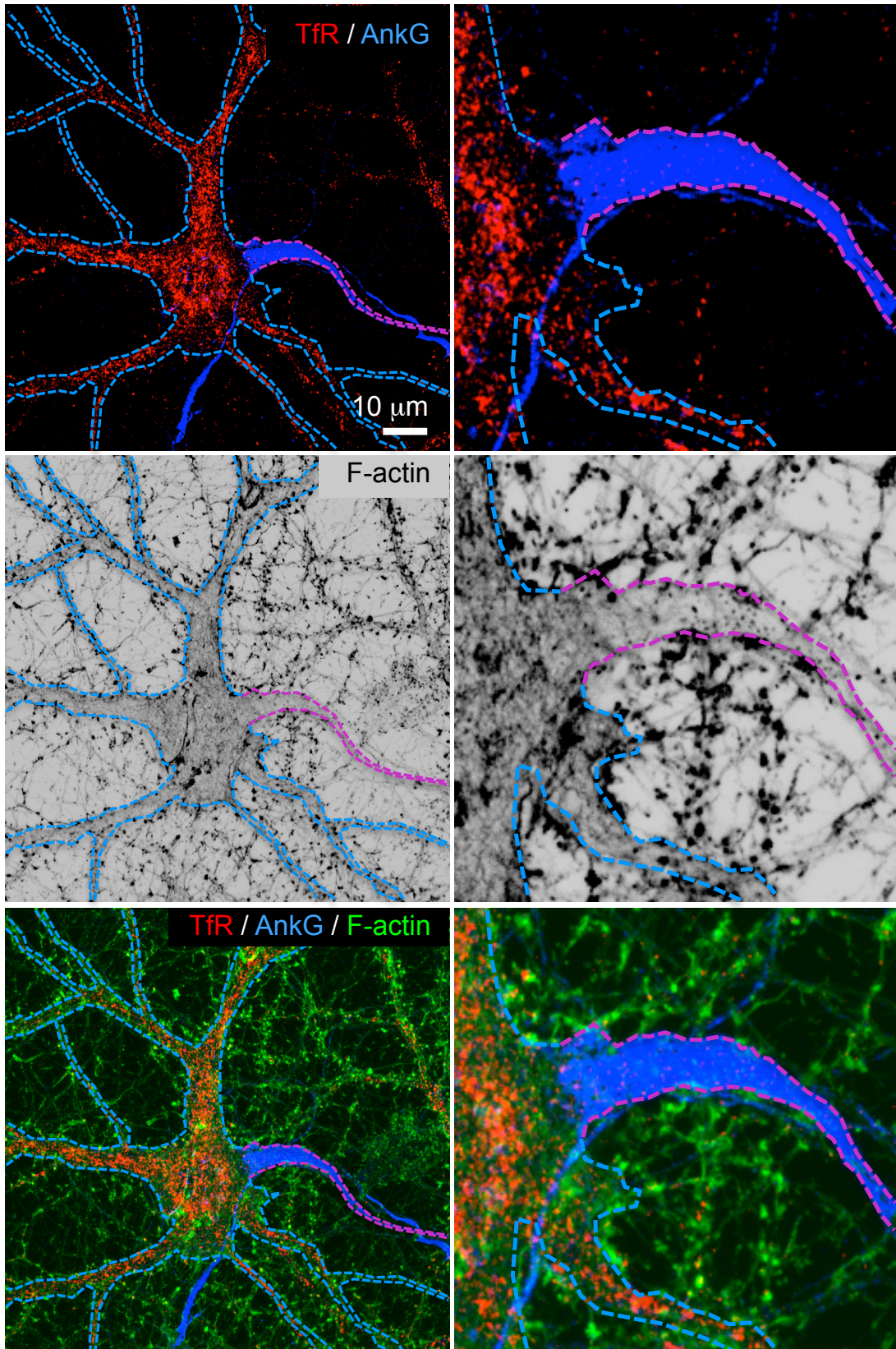


Figure S3

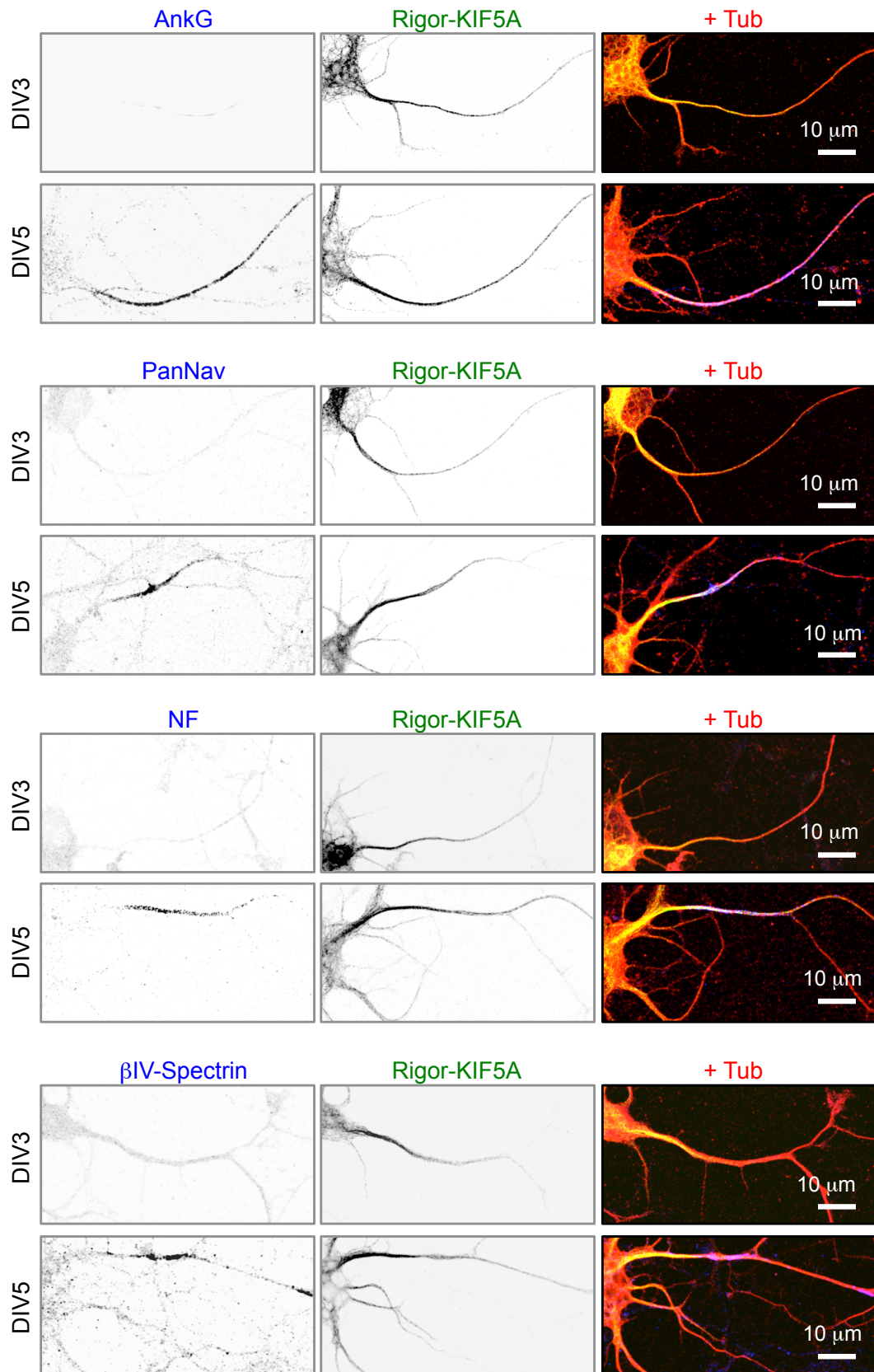


Figure S4

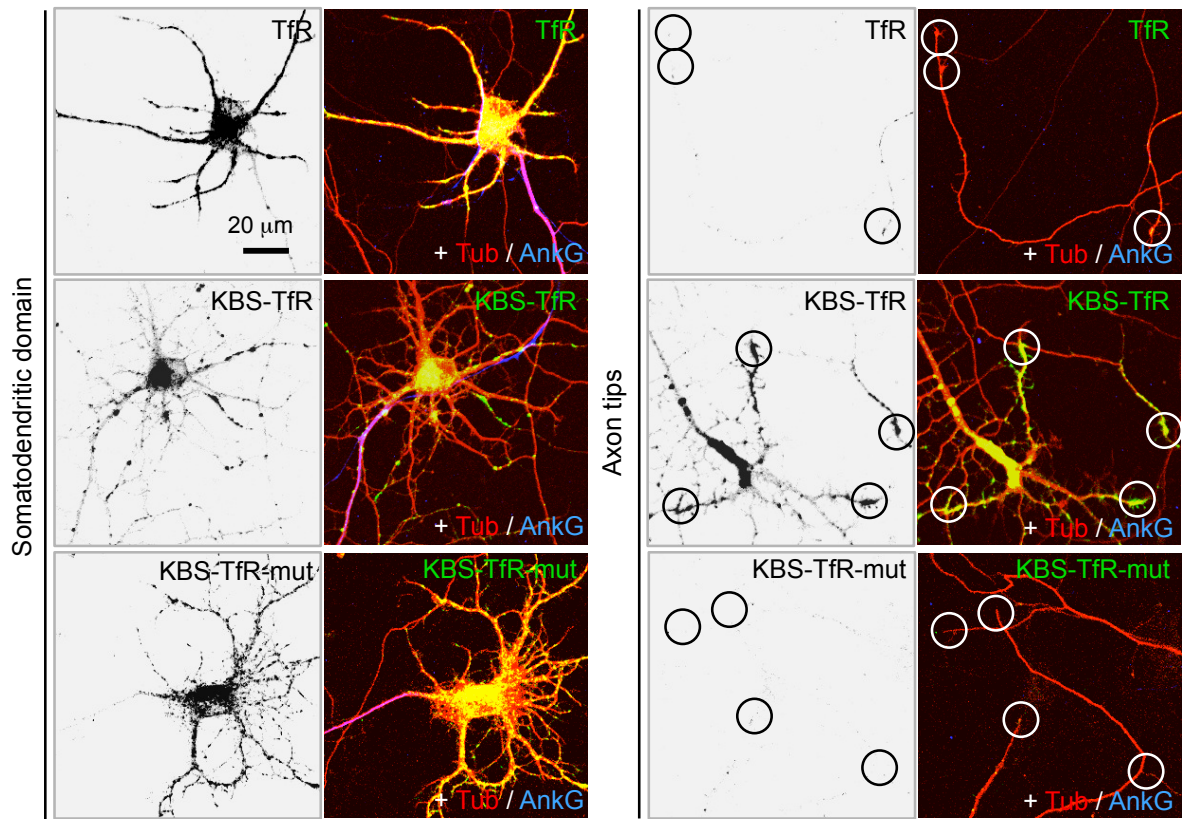


Figure S5

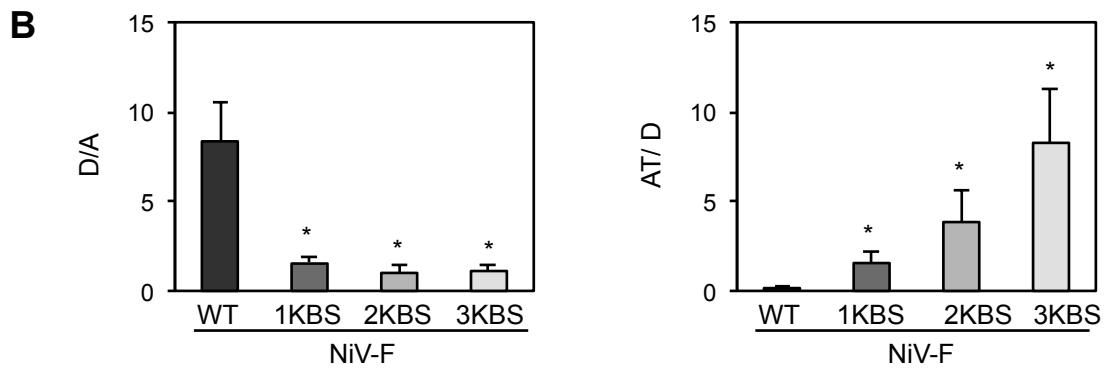
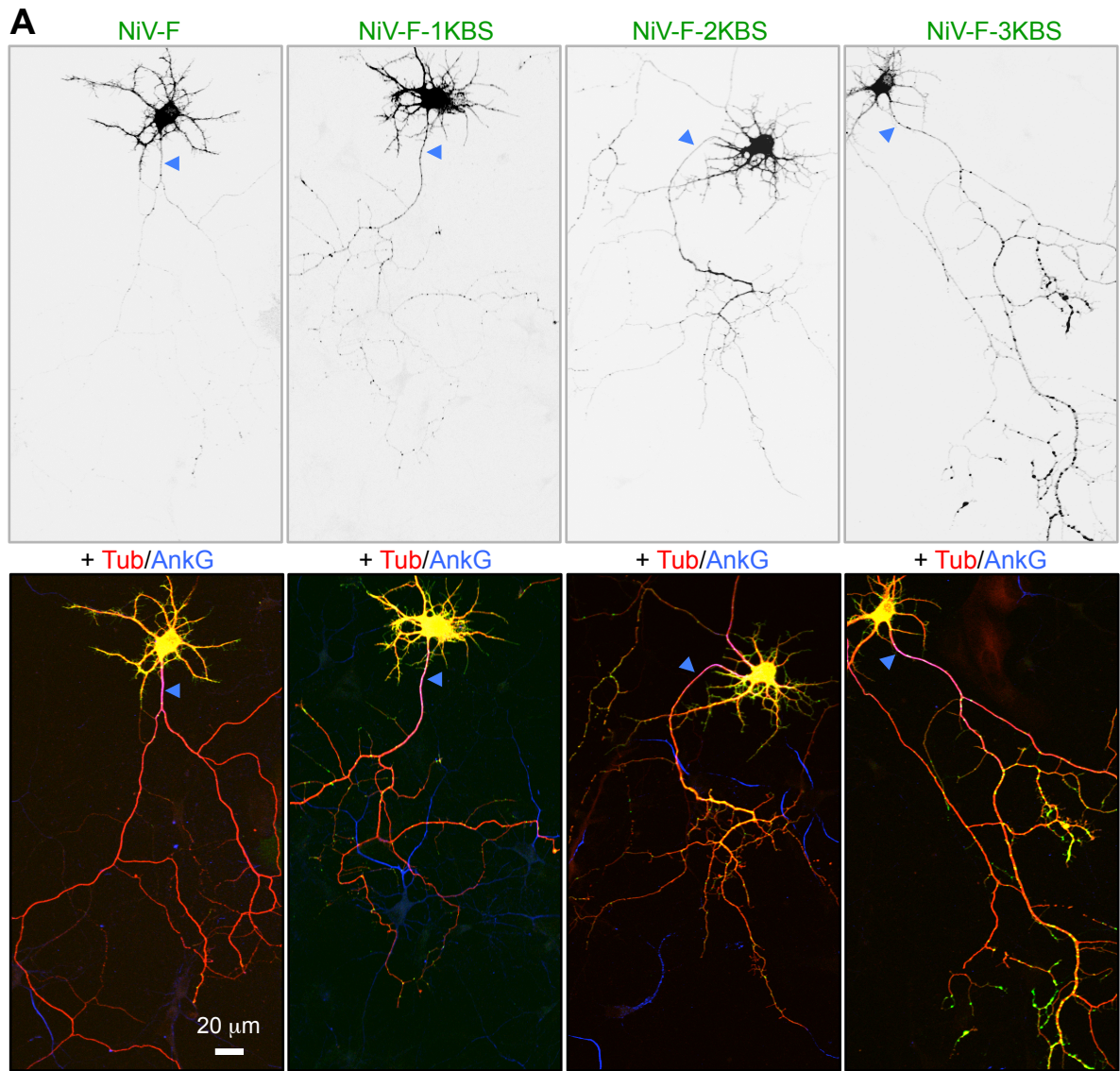


Figure S6

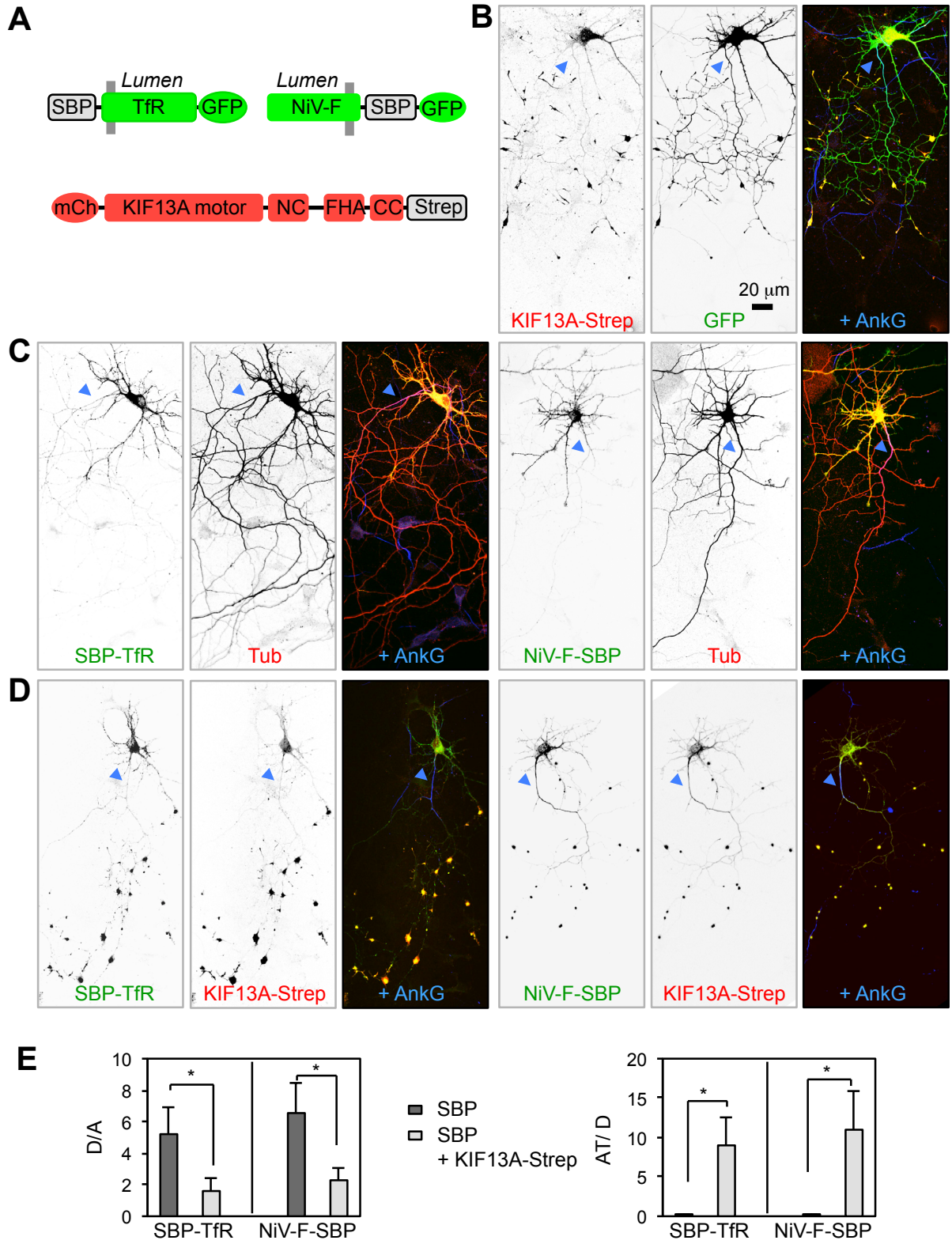
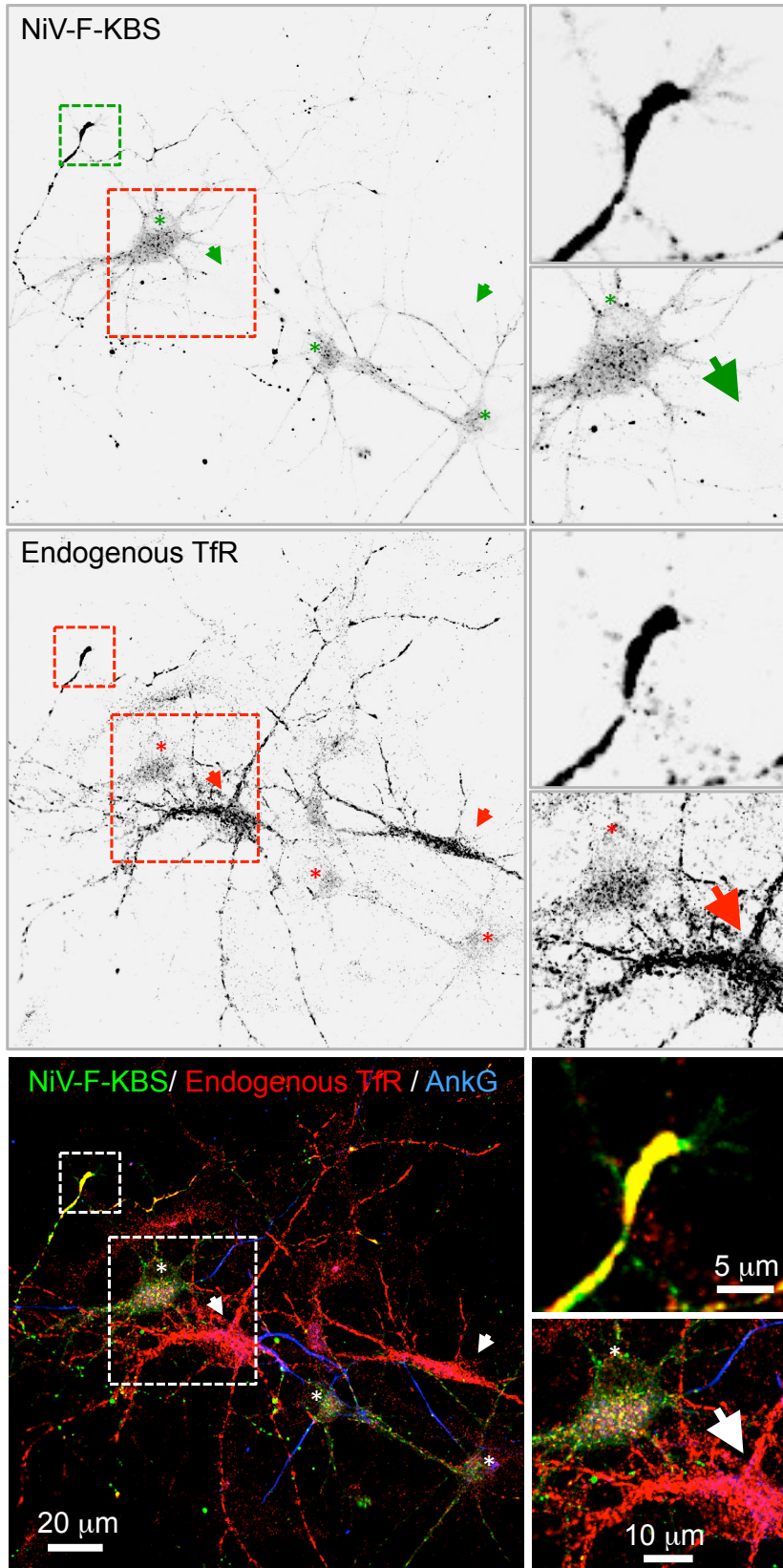


Figure S7



SUPPLEMENTAL FIGURE LEGENDS

Figure S1 (related to Figure 4). Surface TfR is not excluded from the plasma membrane of the PAEZ. DIV10 neurons transfected with a plasmid encoding TfR-GFP (grayscale and green) were stained for surface TfR by incubation of non-permeabilized cells with an antibody to GFP (grayscale and red) and, after fixation-permeabilization, for AnkG (blue) followed by appropriate secondary antibodies. Dashed lines indicate the PAEZ. The punctate staining of surface TfR reflects its localization to clathrin-coated pits.

Figure S2 (related to Figure 4). Absence of dense actin staining at the AIS in mature neurons. Z-stack reconstruction of DIV18 neurons stained for endogenous TfR (red), AnkG (blue) and F-actin (grayscale and green). Enlarged regions are shown on the right panels. Cyan and magenta dashed lines delimit the somatodendritic and axonal areas respectively. Notice the absence of a dense actin structure in the AIS.

Figure S3 (related to Figure 4). Rigor-KIF5A is preferentially recruited to the beginning of axonal microtubules prior to the assembly of the AIS. DIV3 and DIV5 neurons co-expressing GFP-Rigor-KIF5A (grayscale and green) and mCherry-tubulin (Tub) (red) stained for the AIS markers AnkG, PanNav, NF or β IV-Spectrin (grayscale and blue). Notice the preferential binding of Rigor-KIF5A to microtubules directed toward the axon as compared to dendrites before (DIV3) and after (DIV5) assembly of the AIS.

Figure S4 (related to Figure 5). Fusion of a kinesin-light-chain-binding sequence (KBS) to the TfR causes missorting of the chimera to the axon. Enlarged views of the somatodendritic domain (left panels) and axon tips (right panels) corresponding to the neurons in Figure 5B expressing TfR-GFP (upper panels), KBS-TfR-GFP (middle panels) and

KBS-TfR-mut-GFP (bottom panels) in grayscale/green. mCherry-tubulin (Tub) (red) expressed in the same cells was used to highlight both dendrites and axon, and endogenous AnkG staining (blue; appearing magenta in the merged images) to identify the AIS. Axon tips are indicated with circles.

Figure S5 (related to Figure 5). Effect of KBS copy number on missorting of NiV-F-KBS chimeras to the axon. (A) DIV7 neurons co-expressing NiV-F-GFP or NiV-F-KBS-GFP with one, two or three copies of the KBS sequence (grayscale in top row, green in bottom row) and mCherry-tubulin (Tub) (red) were immunostained for AnkG (blue; appearing as magenta in the merged images). Arrowheads point to the AIS. (B) Dendrite/axon (D/A) and axon tip/dendrite (AT/D) ratios of wild-type (WT) NiV-F and NiV-F with one, two or three copies of the KBS sequence. Values are the mean \pm SD from 20 neurons. * $P < 0.001$ relative to WT NiV-F.

Figure S6 (related to Figure 5). Forced interaction with KIF13A redirects SBP-TfR-GFP and NiV-F-SBP-GFP chimeras to the axon.

(A) A streptavidin-binding peptide (SBP) sequence (DEKTTGWRGGHVVEGLAGELEQLRARLEHHPQGQREP) was fused to the cytosolic N-terminus of TfR or C-terminus of NiV-F, both tagged with green fluorescent protein (GFP). Streptavidin (Strep) was fused to the C-terminus of a KIF13A₁₋₆₃₉ fragment comprising the motor, neck coil (NC) and forkhead-associated (FHA) domains plus part of the first coiled coil domain (CC) and tagged at the N-terminus with mCherry. (B) mCherry-KIF13A-Strep (red) distributes to axon tips in DIV7 neurons co-expressing soluble GFP (green). (C) SBP-TfR-GFP (green, left panels) and NiV-F-SBP-GFP (green, right panels) localize to the somatodendritic domain in DIV7 neurons co-expressing mCherry-tubulin (Tub) (red). (D) SBP-TfR-GFP (green, left panels) and NiV-F-SBP-GFP (green, right panels) are redirected to axon tips when co-expressed with mCherry-KIF13A-Strep (red). (B-D) Arrowheads point to

the AIS stained for AnkG (blue). (E) Dendrite/axon (D/A) and axon tip/dendrite (AT/D) ratios of SBP-TfR-GFP and NiV-F-SBP-GFP proteins in neurons co-expressing mCherry-tubulin or mCherry-KIF13A-Strep were quantified from 15 neurons and expressed as mean \pm SD. * $P < 0.001$.

Figure S7 (related to Figure 6). NiV-F-KBS chimera redirects endogenous TfR to axon tips.

DIV10 neurons expressing NiV-F-KBS-GFP (grayscale in upper panels; green in bottom panels) were stained for endogenous TfR (grayscale in middle panels; red in bottom panels) and AnkG (blue in bottom panels). Transfected and untransfected neurons are indicated by asterisks and arrows, respectively. Enlarged regions of an axon tip and soma are shown at the right of each image. Notice that NiV-F-KBS expression causes somatodendritic depletion of endogenous TfR and its accumulation at axon tips.

MOVIE LEGENDS

Movie S1 (related to Figure 2). Axonal exclusion of TfR-GFP-containing anterograde vesicles occurs at the PAEZ. DIV10 neuron expressing TfR-GFP (grayscale on the left panel, green on the right panel) was stained for the AIS with CF555-conjugated antibody to neurofascin (NF) (red on the right panel) and recorded every 500 ms for 120 s. Photobleaching (indicated as PB) was performed after ~5 s of recording to facilitate identification of vesicles entering an axon and a neighboring dendrite. Notice that few TfR-GFP-containing vesicles enter the PAEZ, while many enter the neighboring dendrite. Dendrite (D) and axon (A) are indicated.

Movie S2 (related to Figure 2). Vesicles budding from the Golgi complex enter the dendrites but not the PAEZ. DIV7 neuron co-expressing the ER-hook (Streptavidin-KDEL) and TfR-SBP-GFP (grayscale on the left panel, green on the right panel) and stained for the AIS with CF555-conjugated antibody to neurofascin (NF) (red on the right panel) was incubated with D-biotin for 20 min to release TfR-SBP-GFP from the ER-hook and allow for concentration at the Golgi complex. Cells were then recorded every second for 120 s. The AIS and PAEZ are indicated. Colored arrowheads on the grayscale image trace the trajectories of particles budding from the Golgi complex and moving into dendrites. Notice that most TfR-SBP-GFP vesicles budding from the Golgi complex enter dendrites but not the PAEZ.

Movie S3 (related to Figure 3). Axonal exclusion of somatodendritic vesicles in the absence of the AIS. DIV3 neurons co-transfected with control shRNA or AnkG shRNA together with TfR-GFP (grayscale) and mCherry tubulin (Tub) (red) were stained on DIV8 for the AIS with CF640-conjugated antibody to neurofascin (NF) (blue) to identify neurons expressing AnkG shRNA. Neurons were recorded for TfR-GFP every 500 ms for 120 s. DIV8 neuron expressing control shRNA (left, upper panels) and AnkG shRNA (left, bottom panels) and the respective

enlarged images from axon and dendrites (right panels). Notice that most TfR-GFP vesicles do not enter to the axon in absence of the AIS.

SUPPLEMENTAL EXPERIMENTAL PROCEDURES

Animals

Sprague-Dawley rats (Harlan Laboratories) were temporarily kept at the NIH animal facility. Animal work was conducted under protocol #13-011 following United States regulations and guidelines set forth by the NIH, the Animal Welfare Act, the Guide for the Care and Use of Laboratory Animals, the Public Health Service Policy on Humane Care and Use of Laboratory Animals and the Government Principles for the Utilization and Care of Vertebrate Animals used in Testing, Research and Training.

DNA constructs

Mouse KIF5A cDNA was cloned into pEGFP-C1 (Clontech). Human TfR and NiV-F cDNAs were cloned into pGFP(A206K)-N1 (Clontech), encoding a monomeric GFP variant, as previously described (Farías et al., 2012; Mattera et al., 2014). For construction of KBS-TfR and NiV-F-KBS, sequences encoding one, two or three copies of the kinesin-binding sequence (KBS) TNLEWDDSAI from SKIP (Pernigo et al., 2013; Pu et al., 2015) with a Gly residue between each copy were fused to sequences encoding the cytosolic N-terminus of TfR or C-terminus of NiV-F. Constructs were cloned into the pEGFP-N1 and pmCh-N1 vectors (Clontech). A bicistronic expression plasmid encoding the ER hook (Streptavidin-KDEL; streptavidin fused to a C-terminal ER retention signal Lys-Asp-Glu-Leu) and the reporter ManII-SBP-GFP (Boncompain et al., 2012) were gifts from F. Perez (Institut Curie, Paris, France). TfR-encoding sequences were cloned to replace ManII-encoding sequences in this vector.

For the forced interaction of TfR and NiV-F with KIF13A, sequences encoding a streptavidin-binding peptide (SBP) appended to the N-terminus of TfR or C-terminus of NiV-F were cloned into EGFP(A206K)-N1 (Clontech). An mCherry (mCh)-KIF13A-Strep chimera was generated by cloning sequences encoding the human KIF13A₁₋₆₃₉ fragment

(comprising the motor, neck coil, forkhead-associated and part of the first coiled-coil domain) (Soppina et al., 2014) and streptavidin into the pmCh-C1 vector (Clontech). A 6x(glycine-serine) linker was introduced between the KIF13A and streptavidin sequences to allow freedom of movement between domains. Plasmids encoding other proteins and their sources (in parenthesis) are: AnkG shRNA and control shRNA (Qiagen), mCherry-tubulin and TfR-mCherry (J. Lippincott-Schwartz, NIH, Bethesda, MD); RFP-CLIMP-63 and GFP-RTN (T. Rapoport, Harvard Medical School, Boston, MA); KLC-TPR-HA (K. Verhey, University of Michigan, Ann Arbor, MI); mGluR1-GFP (P. Kammermeier, University of Rochester Medical Center, Rochester, NY); NR2A-GFP (S. Vicini, Georgetown University Medical Center, Washington DC). Amino-acid substitutions in KIF5A-GFP (G235/A) (Rigor-KIF5A), KBS-TfR-GFP (KBS WD/AA), NiV-F-KBS-mCh (KBS WD/AA) and mCherry-tubulin (K40Q) were made by site-directed mutagenesis (QuikChange, Agilent) and verified by DNA sequencing.

Antibodies and other reagents

Rabbit anti-TfR (used at 1:200) and rabbit anti-GM130 (used at 1: 500) were from Abcam. Mouse anti-acetylated tubulin (used at 1:2000) and mouse anti-polyglutamylated tubulin (used at 1:1000) were from Sigma-Aldrich. Mouse anti-AP-1- γ (used at 1:300) and mouse anti-AP-2- α (used at 1:300) were from BD Transduction Laboratories. Goat anti-AnkG (used at 1:50) and rabbit anti-MAP2 (used at 1:300) were from Santa Cruz Biotechnology. Rabbit anti-GluR1 (used at 1:200) was from Millipore Bioscience Research Reagents. Mouse anti-HA (used at 1:1000) was from Covance. Mouse anti-pan-neurofascin (external), Clone A12/18 (used at 1:50), was from the University of California, Davis/NIH NeuroMab Facility. Mouse anti-NgCAM, Clone 8D9 (used at 1:300) made by V. Lemmon was obtained from the Developmental Studies Hybridoma Bank developed under the auspices of the NICHD and maintained by the University of Iowa, Department of Biology, Iowa, IA. Mouse anti-TGN38 (used at 1:500) was a gift from K. Howell, University of Colorado School of Medicine,

Denver, CO. Chicken anti- β IV-spectrin (used at 1:500) was a gift from M. Komada, Tokyo Institute of Technology, Tokyo, Japan. Rabbit anti-GFP and mouse anti-GFP (used at 1:1000), LysoTracker-Red DND-99, MitoTracker-Red-FM, and all secondary antibodies were obtained from Invitrogen. Phalloidin-Alexa405 (used at 1:100), Mix-n-Stain-CF488, Mix-n-Stain-CF555 and Mix-n-Stain-CF640R were from Biotium. The latter three reagents were used to label the antibody to neurofascin. Mix-n-Stain-CF555 was also used to label GFP for the surface staining of TfR-GFP as per the manufacturer's instructions.

Image analysis of fluorescently-labeled cells

Fluorescence line intensity plots: The distribution of different proteins at the transitional zone from the soma (S) to the axon (A) or dendrites (D) was quantified along 1- μ m-wide lines running 10-25 μ m in S \rightarrow A and S \rightarrow D directions in 10-20 neurons. Representative images and their corresponding plots are shown in Figures 1B and 1C, Figure 2E and 2F and Figure 3A and 3B.

Polarity index. The dendrite/axon (D/A) polarity index was quantified as previously described (Farías et al., 2012; Mattera et al., 2014). Briefly, several one-pixel-wide lines were traced along three dendrites and one portion of the axon (not including the AIS) captured in each image. The mean intensities from the three dendrites were averaged and used to calculate the D/A ratio from a total of 25 neurons. D/A=1 represents non-polarized distribution; D/A>1, preferential dendritic localization; D/A<1, preferential axonal localization. For calculation of the D/A index of endogenous TfR shown in Figure 1E, AnkG immunostaining and phalloidin were used to mark the AIS and all neurites, respectively, except for DIV2-3, when the axon was identified as the longest neurite stained with phalloidin-Alexa405, because of the absence of AnkG expression (Figure 1F). For experiments using AnkG shRNA or control shRNA shown in Figure 3, one-pixel-wide lines were traced along the first 30 μ m of each axon stained for the AIS marker AnkG. Knocking down of AnkG was calculated from 20 neurons and expressed as percentage. The total and surface

TfR-GFP D/A indexes were calculated similarly to the endogenous TfR D / A polarity index from 20 neurons for each one. For experiments using chimeras shown in Figures 5, 6, 7, S4, S5 and S6 the D/A and axon-tips/dendrite (AT/D) indexes were calculated similarly to the endogenous TfR D/A polarity index. Several one-pixel-wide lines were traced along three axon tips and three dendrites corresponding to the same transfected neuron and averaged to calculate AT/D ratios for each neuron. A total of 15-25 neurons were quantified for each condition. AT/D ratio >1 represents axon tip accumulation; <1 preferential dendritic accumulation. Axon tips were identified by staining for endogenous polyglutamylated tubulin at the end of axons marked by mCh-tubulin expression.

AIS and PAEZ areas. To quantify the AIS area indicated in Figure 1E, the area stained for AnkG was delimited by freehand selection for each neuron. An average area was calculated from a total of 25 AIS corresponding to 25 different neurons. The PAEZ area shown in Figure 1E was calculated similarly to the AIS area, except that it was selected in merged images of TfR and AnkG staining as a zone devoid of both proteins. Because of the absence of AnkG at DIV2-3, it was not possible determine the area of the AIS and PAEZ at this stage of neuronal development in culture.

Quantification of live-cell imaging

Movement of particles containing TfR-GFP was quantified using ImageJ version 1.44o. Lines (20-pixel-wide, 35-mm-long) were traced from the soma to the axon (S→A) and from the soma to the dendrites (S→D) in photobleached regions from 15 neurons (as shown in Figure 2B). Kymographs were generated from straightened lines by re-slicing stacks followed by z-projection. (S→A) and (S→D) tracks were orientated so that anterograde movement occurred from left to right. The number of anterograde particles entering the dendrites and axons was determined manually from kymographs. Quantification of the number of particles moving from soma to axon was subdivided into the PAEZ and the AIS regions. The PAEZ was defined as a region 5- μ m proximal to the edge of the AIS stained by anti-NF-CF555. To

compare anterograde transport to the axon versus dendrites, the total number of particles (100 %) was considered to be [(S→PAEZ) + (S→AIS) + (S→D)]. The trajectory of particles entering the PAEZ/ AIS was monitored regardless of whether they stopped and returned to the soma or continued to distal parts of the axon. Anterograde movement followed by stoppage and retrograde transport to the soma was observed as loops in kymographs at the PAEZ (Figure 2C). The total number of particles analyzed is indicated in Figure 2H.

Anterograde transport of particles containing TfR-SBP-GFP from the TGN to axon and dendrites was determined manually. Because of the small number of particles budding from the TGN, three different S→D tracks were quantified and averaged to compare with the S→A track for each neuron. Quantification of the number of particles moving from soma to axon was subdivided into the PAEZ and the AIS and represented as percentage, similar to TfR-GFP vesicle transport described above. A total of 15 neurons were analyzed. The total number of particles (n) analyzed is indicated in Figure 2L.

Statistical Methods

All the pooled data are presented as the mean \pm SD or the percentage \pm SEM as indicated in each figure legend from at least three independent experiments. Two-tailed Student's t test for unpaired data was used to evaluate single comparisons between different experimental groups using Microsoft Excel. Differences were considered statistically significant for a value of $P < 0.001$. n.s. not significant.

SUPPLEMENTAL REFERENCES

- Boncompain, G., Divoux, S., Gareil, N., de Forges, H., Lescure, A., Latreche, L., Mercanti, V., Jollivet, F., Raposo, G., and Perez, F. (2012). Synchronization of secretory protein traffic in populations of cells. *Nat Methods* 9, 493-498.
- Farías, G. G., Cuitiño, L., Guo, X., Ren, X., Jarnik, M., Mattera, R., and Bonifacino, J. S. (2012). Signal-Mediated, AP-1/Clathrin-Dependent Sorting of Transmembrane Receptors to the Somatodendritic Domain of Hippocampal Neurons. *Neuron* 75, 810-823.
- Mattera, R., Farías, G. G., Mardones, G. A., and Bonifacino, J. S. (2014). Co-assembly of viral envelope glycoproteins regulates their polarized sorting in neurons. *PLoS Pathog* 10, e1004107.
- Pernigo, S., Lamprecht, A., Steiner, R. A., and Dodding, M. P. (2013). Structural basis for kinesin-1:cargo recognition. *Science* 340, 356-359.
- Pu, J., Schindler, C., Jia, R., Jarnik, M., Backlund, P., and Bonifacino, J. S. (2015). BORC, a multisubunit complex that regulates lysosome positioning. *Dev. Cell*, in press.
- Soppina, V., Norris, S.R., Dizaji, A.S., Kortus, M., Veatch, S., Peckham, M., Verhey, K.J. (2014) Dimerization of mammalian kinesin-3 motors results in superprocessive motion. *Proc Natl Acad Sci U S A*. 111, 5562-5567.